# PATH FOLLOWING SOLUTION APPROACHES AND INTEGRATION OF CONSTITUTIVE RELATIONS FOR A 3D WOOD COHESIVE ZONE MODEL

HENRIK DANIELSSON

# PATH FOLLOWING SOLUTION APPROACHES AND INTEGRATION OF CONSTITUTIVE RELATIONS FOR A 3D WOOD COHESIVE ZONE MODEL

HENRIK DANIELSSON

# Path following solution approaches and integration of constitutive relations for a 3D wood cohesive zone model

Henrik Danielsson

## Abstract

A nonlinear finite element formulation for material nonlinearity is presented based on assumptions of small strains and neglecting geometrically nonlinear effects. The Euler forward approach, the Newton-Raphson approach and a path-following approach for solving the global nonlinear equations are presented. The considered path-following approach is the arc-length method, for which different types of constraint equations found in the literature are presented. A method for determining the stress based on numerical integration of incremental constitutive relations for an elasto-plastic material is also presented. The considered material model is a 3D cohesive zone model, developed to enable perpendicular to grain fracture analysis of wood.

## Contents

# 1 Introduction

The theory presented here relates to nonlinear finite element formulation with respect to material nonlinearity, some different procedures for solving the nonlinear equations of equilibrium and a procedure to determine current stress state based on numerical integration of incremental constitutive relations. The aim of the presentation is to give the relevant theoretical background regarding the numerical implementation of a 3D wood cohesive zone model based on theory of plasticity, presented in [4]. The material model is implemented for finite element analysis in MATLAB [7] using supplementary routines from the toolbox CALFEM [1] and is in [4], [5] and [6] used for perpendicular to grain fracture analysis of various wooden structural elements.

The theory presented in Sections 2, 3 and 4 regarding nonlinear finite element formulation and solution approaches does not represent original research carried out by the author but represents common text book approaches regarding the considered areas and is based on [3], [8], [9] and [10]. In Section 5, the cohesive zone model presented in [4] is briefly reviewed and considered with respect to numerical integrations of the incremental constitutive relations. The considered method for the numerical integrations is according to [9]. The notation used here is partly changed with respect to the above given references. In the following presentation, geometrical nonlinear effects are neglected and the assumption of small strains is used.

# 2 Equations of motion - strong and weak forms

Consider a body, or an arbitrary part of a body, of volume $\Omega$ with boundary $S$ and an outward unit normal vector $\mathbf{n}$ according to Figure 1. The forces acting on this body are given by the traction vector $\mathbf{t}$ acting on the surface $S$ and the body forces $\mathbf{b}$ per unit volume in $\Omega$. The displacement is denoted $\mathbf{u}$ and the acceleration is represented by $\ddot{\mathbf{u}}$, i.e. the second derivative of $\mathbf{u}$ with respect to time. Newton's second law of motion states that

$$\int_S \mathbf{t}\, \mathrm{d}S + \int_\Omega \mathbf{b}\, \mathrm{d}\Omega = \int_\Omega \rho \ddot{\mathbf{u}}\, \mathrm{d}\Omega \quad \text{where} \quad \mathbf{t} = \begin{bmatrix} t_x \\ t_y \\ t_z \end{bmatrix}, \quad \mathbf{b} = \begin{bmatrix} b_x \\ b_y \\ b_z \end{bmatrix}, \quad \mathbf{u} = \begin{bmatrix} u_x \\ u_y \\ u_z \end{bmatrix} \quad (1)$$

and where $\rho$ is the mass density. The traction vector $\mathbf{t}$ for a surface with an outward normal vector $\mathbf{n}$ is related to the stress tensor $\mathbf{S}$ according to

$$\mathbf{t} = \mathbf{S}\mathbf{n} \quad \text{where} \quad \mathbf{S} = \begin{bmatrix} \sigma_{xx} & \tau_{xy} & \tau_{xz} \\ \tau_{yx} & \sigma_{yy} & \tau_{yz} \\ \tau_{zx} & \tau_{zy} & \sigma_{zz} \end{bmatrix}, \quad \mathbf{n} = \begin{bmatrix} n_x \\ n_y \\ n_z \end{bmatrix} \quad (2)$$

and where $\mathbf{S}$ is symmetric, i.e. $\mathbf{S} = \mathbf{S}^T$, since $\tau_{xy} = \tau_{yx}$, $\tau_{xz} = \tau_{zx}$ and $\tau_{yz} = \tau_{zy}$ due to rotational equilibrium reasons.
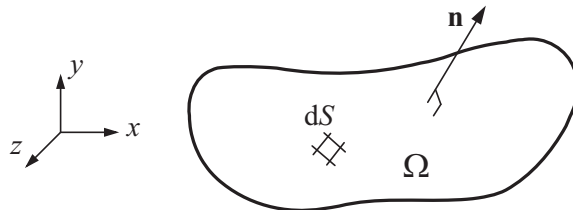


Figure 1: Body of volume $\Omega$ with surface $S$.

The stress vector $\boldsymbol{\sigma}$ and the matrix differential operator $\tilde{\nabla}$ are further introduced according to

$$\boldsymbol{\sigma} = \begin{bmatrix} \sigma_{xx} \\ \sigma_{yy} \\ \sigma_{zz} \\ \tau_{xy} \\ \tau_{xz} \\ \tau_{yz} \end{bmatrix} \quad \text{and} \quad \tilde{\nabla} = \begin{bmatrix} \frac{\partial}{\partial x} & 0 & 0 \\ 0 & \frac{\partial}{\partial y} & 0 \\ 0 & 0 & \frac{\partial}{\partial z} \\ \frac{\partial}{\partial y} & \frac{\partial}{\partial x} & 0 \\ \frac{\partial}{\partial z} & 0 & \frac{\partial}{\partial x} \\ 0 & \frac{\partial}{\partial z} & \frac{\partial}{\partial y} \end{bmatrix} \tag{3}$$

Using the divergence theorem of Gauss, Newton's second law of motion according to Equation (1) may then be expressed as

$$\int_{\Omega} \left( \tilde{\nabla}^T \boldsymbol{\sigma} + \mathbf{b} - \rho \ddot{\mathbf{u}} \right) \, \mathrm{d}\Omega = 0 \tag{4}$$

from which the *strong form* of the equations of motion may be found as

$$\tilde{\nabla}^T \boldsymbol{\sigma} + \mathbf{b} = \rho \ddot{\mathbf{u}} \tag{5}$$

since the considered volume $\Omega$ is arbitrary. An arbitrary vector $\mathbf{v}$ - the weight vector - is introduced to arrive at the weak form. Multiplying Equation (5) with $\mathbf{v}$, integrating over the volume $\Omega$ and using the divergence theorem of Gauss the *weak form* of the equations of motion may be obtained as

$$\int_{\Omega} \rho \mathbf{v}^T \ddot{\mathbf{u}} \, \mathrm{d}\Omega + \int_{\Omega} (\tilde{\nabla} \mathbf{v})^T \boldsymbol{\sigma} \, \mathrm{d}\Omega = \int_{S} \mathbf{v}^T \mathbf{t} \, \mathrm{d}S + \int_{\Omega} \mathbf{v}^T \mathbf{b} \, \mathrm{d}\Omega \quad \text{where} \quad \mathbf{v} = \begin{bmatrix} v_x \\ v_y \\ v_z \end{bmatrix} \tag{6}$$

The weak form may be modified for further preparations for the finite element formulation. A quantity $\boldsymbol{\varepsilon}^v$ is defined, related to the weight vector $\mathbf{v}$ in the same manner as the small strain vector $\boldsymbol{\varepsilon}$ is related to the displacement vector $\mathbf{u}$, i.e. according to the kinematic relation

$$\boldsymbol{\varepsilon} = \begin{bmatrix} \varepsilon_{xx} & \varepsilon_{yy} & \varepsilon_{zz} & \gamma_{xy} & \gamma_{xz} & \gamma_{yz} \end{bmatrix}^T = \tilde{\nabla} \mathbf{u} \quad \text{and} \quad \boldsymbol{\varepsilon}^v = \tilde{\nabla} \mathbf{v} \tag{7}$$

with the matrix differential operator $\tilde{\nabla}$ defined in Equation (3). The weak form may hence be expressed as

$$\int_{\Omega} \rho \mathbf{v}^T \ddot{\mathbf{u}} \, \mathrm{d}\Omega + \int_{\Omega} (\boldsymbol{\varepsilon}^v)^T \boldsymbol{\sigma} \, \mathrm{d}\Omega = \int_{S} \mathbf{v}^T \mathbf{t} \, \mathrm{d}S + \int_{\Omega} \mathbf{v}^T \mathbf{b} \, \mathrm{d}\Omega \tag{8}$$

Interpretation of the weight vector $\mathbf{v}$ as a virtual displacement and hence $\boldsymbol{\varepsilon}^v$ as the related virtual strain, Equation (8) may be referred to as the *principle of virtual work* where the right hand side represents the external work during a virtual displacement $\mathbf{v}$. The strong and weak forms of the equations of motion are derivable from one another. An advantage in favor of the weak form is that it includes no derivatives of the stress tensor, which makes it suitable as a base for finite element formulations.

Both the strong and the weak form of the equations of motion hold for all constitutive relations. In order to solve a specific boundary value problem also the boundary conditions are needed with $\mathbf{u}$ given along the boundary $S_u$ and $\mathbf{t}$ given along the boundary $S_t$.

# 3 Finite element formulation

The finite element formulation will be presented for static conditions only, i.e. $\ddot{\mathbf{u}} = 0$. With this restriction, the weak form of the equations of motion in Equation (8) turns to the weak form of the equations of equilibrium according to

$$\int_\Omega (\boldsymbol{\varepsilon}^v)^T \boldsymbol{\sigma} \, \mathrm{d}\Omega = \int_S \mathbf{v}^T \mathbf{t} \, \mathrm{d}S + \int_\Omega \mathbf{v}^T \mathbf{b} \, \mathrm{d}\Omega \tag{9}$$

In the finite element formulation, the displacement vector $\mathbf{u}$ is throughout the body approximated by the nodal displacements and shape functions according to

$$\mathbf{u} \approx \mathbf{Na} \tag{10}$$

where $\mathbf{N}$ is the global shape function matrix and $\mathbf{a}$ is the nodal displacement vector containing $n_{dof}$ nodal displacements. The strains $\boldsymbol{\varepsilon}$ are then given by the following strain-nodal displacement relationship

$$\boldsymbol{\varepsilon} = \mathbf{Ba} \qquad \text{where} \quad \mathbf{B} = \tilde{\nabla}\mathbf{N} \tag{11}$$

The fundamental issue of the standard finite element method is that the arbitrary weight vector $\mathbf{v}$ is chosen according to Galerkin's method, i.e. according to

$$\mathbf{v} = \mathbf{Nc} \tag{12}$$

where since $\mathbf{v}$ is arbitrary, also $\mathbf{c}$ is arbitrary. The quantity $\boldsymbol{\varepsilon}^v$, related to the weight vector $\mathbf{v}$ as the strain $\boldsymbol{\varepsilon}$ is related to the displacement $\mathbf{u}$, is hence given by

$$\boldsymbol{\varepsilon}^v = \mathbf{Bc} \tag{13}$$

Use of Equations (12) and (13) in the weak form of the equations of equilibrium given in Equation (9) yields

$$\int_\Omega \mathbf{c}^T \mathbf{B}^T \boldsymbol{\sigma} \, \mathrm{d}\Omega = \int_S \mathbf{c}^T \mathbf{N}^T \mathbf{t} \, \mathrm{d}S + \int_\Omega \mathbf{c}^T \mathbf{N}^T \mathbf{b} \, \mathrm{d}\Omega \tag{14}$$

and since the vector $\mathbf{c}$ is independent of position in the body and arbitrary we may finally obtain

$$\int_\Omega \mathbf{B}^T \boldsymbol{\sigma} \, \mathrm{d}\Omega - \int_S \mathbf{N}^T \mathbf{t} \, \mathrm{d}S - \int_\Omega \mathbf{N}^T \mathbf{b} \, \mathrm{d}\Omega = \mathbf{0} \tag{15}$$

The finite element formulation of the equations of equilibrium may hence be expressed as

$$\mathbf{G} = \mathbf{f}_{int} - \mathbf{f}_{ext} = \mathbf{0} \tag{16}$$

where $\mathbf{G}$ is the residual force vector (or the out-of-balance force vector) and where the internal force vector $\mathbf{f}_{int}$ and the external force vector $\mathbf{f}_{ext}$ are given by

$$\mathbf{f}_{int} = \int_\Omega \mathbf{B}^T \boldsymbol{\sigma} \, \mathrm{d}\Omega \tag{17}$$

$$\mathbf{f}_{ext} = \int_S \mathbf{N}^T \mathbf{t} \, \mathrm{d}S + \int_\Omega \mathbf{N}^T \mathbf{b} \, \mathrm{d}\Omega \tag{18}$$

and hence expresses that the internal and external forces must balance each other. The above equations of equilibrium hold irrespective of the constitutive relation. However, to solve a specific boundary value problem, a constitutive relation needs to be defined and also boundary conditions need to be specified. For linear elasticity with a constitutive relation defined by Hooke's law we have with Equation (11) that

$$\boldsymbol{\sigma} = \mathbf{D}\boldsymbol{\varepsilon} = \mathbf{D}\mathbf{B}\mathbf{a} \tag{19}$$

and the linear equations of equilibrium are given by

$$\mathbf{K}\mathbf{a} = \mathbf{f}_{ext} \qquad \text{where} \quad \mathbf{K} = \int_{\Omega} \mathbf{B}^T \mathbf{D}\mathbf{B} \, \mathrm{d}\Omega \tag{20}$$

where the linear elastic stiffness matrix $\mathbf{K}$ is constant.

# 4 Solution of nonlinear equations of equilibrium

The solution procedure for nonlinear material behavior is more complex compared to that of linear elasticity, since the current stress is generally not possible to obtain directly from the current strain. For many types of material nonlinearity, including plasticity, the constitutive relation is given in an incremental form and the current stress needs to be found by integration of this incremental constitutive relation along the load path. There are hence two sets of nonlinear equations to be dealt with: one related to the global equations of equilibrium and one related to the local constitutive relation at the material point level.

Considering elasto-plasticity, the incremental constitutive relation may be described as

$$\dot{\boldsymbol{\sigma}} = \mathbf{D}_t \dot{\boldsymbol{\varepsilon}} \qquad \text{where} \quad \mathbf{D}_t = \begin{cases} \mathbf{D} & \text{for elastic response} \\ \mathbf{D}^{ep} & \text{for elasto-plastic response} \end{cases} \tag{21}$$

where $(\dot{*})$ denotes incremental quantities and $\mathbf{D}_t$ is the tangential material stiffness matrix, equal to the linear elastic stiffness matrix $\mathbf{D}$ if the response is purely elastic or else equal to the elasto-plastic tangential stiffness matrix $\mathbf{D}^{ep}$.

The nature of this type of problems requires an incremental solution technique, where the response is tracked by applying the external loading in small steps. The demand on the solution procedures for both sets of nonlinear equations is that it should be sufficiently accurate and efficient. Solution techniques for the global equations of equilibrium will be dealt with in this section whereas the a procedure for solving the local equations, i.e. the integration of constitutive relations, will be dealt with in Section 5.

## 4.1 Euler forward solution scheme

For solving the global equations of equilibrium in an incremental fashion, the *Euler forward* scheme is one of the simplest schemes at hand. The Euler forward scheme is based on the assumption that the tangent stiffness between a known point $n$ on the load path and the next sought point $n+1$ may be approximated by the tangent stiffness at $n$. To obtain the formulation of the Euler forward scheme, the global equations of equilibrium according to Equation (16) are differentiated yielding

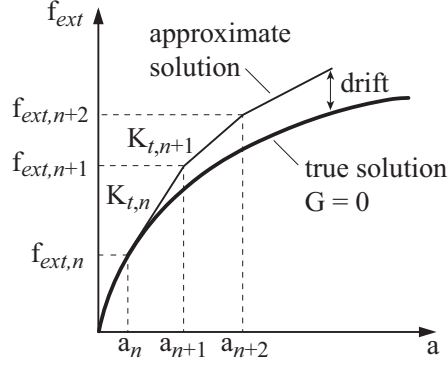$$\dot{\mathbf{f}}_{int} - \dot{\mathbf{f}}_{ext} = \mathbf{0} \tag{22}$$

Figure 2: Illustration of Euler forward solution scheme.

where

$$\dot{\mathbf{f}}_{int} = \int_{\Omega} \mathbf{B}^T \dot{\boldsymbol{\sigma}} \; \mathrm{d}\Omega \qquad \text{and} \qquad \dot{\mathbf{f}}_{ext} = \int_{S} \mathbf{N}^T \dot{\mathbf{t}} \; \mathrm{d}S + \int_{\Omega} \mathbf{N}^T \dot{\mathbf{b}} \; \mathrm{d}\Omega \qquad (23)$$

Using the incremental constitutive relation according to Equation (21) and the finite element approximation of the strain-nodal displacement relation according to Equation (11) yields

$$\dot{\boldsymbol{\sigma}} = \mathbf{D}_t \dot{\boldsymbol{\varepsilon}} = \mathbf{D}_t \mathbf{B} \dot{\mathbf{a}} \qquad (24)$$

and the global equations of equilibrium may hence be expressed in incremental form as

$$\mathbf{K}_t \dot{\mathbf{a}} = \dot{\mathbf{f}}_{ext} \qquad \text{where} \quad \mathbf{K}_t = \int_{\Omega} \mathbf{B}^T \mathbf{D}_t \mathbf{B} \; \mathrm{d}\Omega \qquad (25)$$

where $\mathbf{K}_t$ represent the current tangential stiffness. All quantities are assumed to be known at state $n$, and the quantities at the next state $n + 1$ are sought. Assuming that the tangential stiffness $\mathbf{K}_t$ is constant between these two states, approximations of the sought quantities may be found by first integrating Equation (25) from state $n$ to state $n + 1$ yielding

$$\mathbf{K}_{t,n}(\mathbf{a}_{n+1} - \mathbf{a}_n) = \mathbf{f}_{ext,n+1} - \mathbf{f}_{ext,n} \qquad \text{where} \quad \mathbf{K}_{t,n} = \int_{\Omega} \mathbf{B}^T \mathbf{D}_{t,n} \mathbf{B} \; \mathrm{d}\Omega \qquad (26)$$

and solving the sought nodal displacements $\mathbf{a}_{n+1}$ for the load $\mathbf{f}_{ext,n+1}$, considering the essential boundary conditions. This in turn allows for determination of the strains $\boldsymbol{\varepsilon}_{n+1}$, the stresses $\boldsymbol{\sigma}_{n+1}$ and the internal forces $\mathbf{f}_{int}$ that these stresses give rise to. The calculated internal forces $\mathbf{f}_{int}$ do not necessarily balance the external forces $\mathbf{f}_{ext}$ when the Euler forward scheme is used, meaning that the out-of-balance force vector $\mathbf{G}$ may be nonzero and equilibrium hence not fulfilled. This imbalance may introduce a drift of the approximate solution from the true solution, as is illustrated in Figure 2.

The Euler forward scheme does however have the positive features of being simple and robust. Using a formulation where loading is applied as prescribed displacements, a possible post peak-load softening part of the load path may also be followed.

## 4.2 Newton-Raphson solution scheme

Among the incremental-iterative solution schemes, the *Newton-Raphson* scheme is one of the most widely used when it comes to nonlinear finite element analysis. In contrast to the Euler forward schemes, where global equilibrium is not necessarily fulfilled, the Newton-Raphson

procedure aims at fulfilling the global equilibrium equations. The basic concept of the Newton-Raphson scheme is to linearize the nonlinear equations of equilibrium about a given point on the load path. The nonlinear equations are approximated by a Taylor expansion, where terms higher than the linear ones are ignored.

The nonlinear global equations of equilibrium according to Equation (16) may for a fixed external loading be expressed as

$$\mathbf{G}(\mathbf{a}) = \mathbf{f}_{int}(\mathbf{a}) - \mathbf{f}_{ext} = \mathbf{0} \tag{27}$$

since the external forces $\mathbf{f}_{ext}$ are known and fixed and since the internal forces depend on the stresses $\boldsymbol{\sigma}$ which in turn depend on the nodal displacements $\mathbf{a}$. Assuming that an approximate solution $\mathbf{a}^{i-1}$ to the true solution $\mathbf{a}$ has been established, the truncated Taylor expansion of $\mathbf{G}$ about $\mathbf{a}^{i-1}$ yields

$$\mathbf{G}(\mathbf{a}^i) = \mathbf{G}(\mathbf{a}^{i-1}) + \left(\frac{\partial \mathbf{G}}{\partial \mathbf{a}}\right)^{i-1} (\mathbf{a}^i - \mathbf{a}^{i-1}) \tag{28}$$

where the derivative $\partial \mathbf{G}/\partial \mathbf{a}$ is found to be

$$\frac{\partial \mathbf{G}}{\partial \mathbf{a}} = \frac{\partial \mathbf{f}_{int}}{\partial \mathbf{a}} = \int_\Omega \mathbf{B}^T \frac{d\boldsymbol{\sigma}}{d\mathbf{a}} \, d\Omega = \int_\Omega \mathbf{B}^T \mathbf{D}_t \mathbf{B} \, d\Omega \tag{29}$$

since $d\boldsymbol{\sigma} = \mathbf{D}_t d\boldsymbol{\varepsilon} = \mathbf{D}_t \mathbf{B} d\mathbf{a}$ and since the external forces $\mathbf{f}_{ext}$ are known and fixed. The derivative $\partial \mathbf{G}/\partial \mathbf{a}$ is hence the tangential stiffness matrix which also emerged in the Euler forward scheme, see Equation (25). Enforcing $\mathbf{G}(\mathbf{a}^i) = \mathbf{0}$, the Newton-Raphson iteration scheme may hence from Equation (28) be expressed as

$$\mathbf{K}_t^{i-1}(\mathbf{a}^i - \mathbf{a}^{i-1}) = -\mathbf{G}(\mathbf{a}^{i-1}) \qquad \text{where} \quad \mathbf{K}_t^{i-1} = \int_\Omega \mathbf{B}^T \mathbf{D}_t^{i-1} \mathbf{B} \, d\Omega \tag{30}$$

where $(*)^{i-1}$ refer to known quantities and the sought nodal displacements $\mathbf{a}^i$ may be solved for, considering the essential boundary conditions. Assuming that $n$ is a known equilibrium state with known nodal displacements $\mathbf{a}_n$, stresses $\boldsymbol{\sigma}_n$ and external forces $\mathbf{f}_{ext,n}$ the aim of the iteration procedure is to find the corresponding quantities for the next state $n+1$, fulfilling the equations of equilibrium. Since the external forces at state $n+1$ are fixed and given by $\mathbf{f}_{ext,n+1}$, the out-of-balance forces $\mathbf{G}(\mathbf{a}^{i-1})$ are given by

$$\mathbf{G}(\mathbf{a}^{i-1}) = \int_\Omega \mathbf{B}^T \boldsymbol{\sigma}^{i-1} \, d\Omega - \mathbf{f}_{ext,n+1} \tag{31}$$

For the first iteration in a load step, when $i = 1$, the starting values are taken as the last known values at equilibrium according to

$$\mathbf{a}^0 = \mathbf{a}_n \, , \qquad \boldsymbol{\varepsilon}^0 = \boldsymbol{\varepsilon}_n \, , \qquad \boldsymbol{\sigma}^0 = \boldsymbol{\sigma}_n \, , \qquad \mathbf{K}_t^0 = \mathbf{K}_{t,n} \tag{32}$$

and the iteration procedure continues until the difference between the external forces $\mathbf{f}_{ext}$ and the internal forces $\mathbf{f}_{int}$ is sufficiently small, i.e. until some norm of the out-of-balance forces $\mathbf{G}(\mathbf{a})$ fulfills a user specified convergence criterion. When equilibrium is reached with sufficient accuracy, the updated equilibrium quantities are accepted as converged equilibrium quantities.

There are variations of the conventional Newton-Raphson scheme (often denoted the *Full Newton-Raphson* scheme) presented above and illustrated in Figure 3. Such variations include
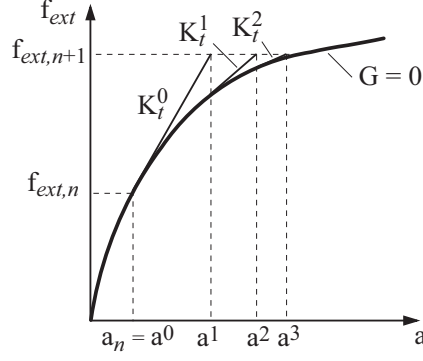
Figure 3: Illustration Newton-Raphson solution scheme.

the *Initial stiffness method*, where the initial linear elastic stiffness is used instead of the tangential stiffness, and the *Modified Newton-Raphson* method, where the tangential stiffness is updated not in every iteration but only once in each load step.

The Newton-Raphson scheme does in general provide a fast convergence and works well in both loading and unloading [9]. Using a formulation where loading is applied as prescribed displacements, a possible post peak-load softening part of the load path may also be followed. The Newton-Raphson scheme does however not manage snap-back behavior of the load path.

## 4.3 Path following solution schemes – arc-length methods

For the case when the load path includes snap-back, which cannot be followed using a Newton-Raphson scheme, a path following scheme such as the *arc-length method* needs to be employed. The procedure presented here is based on the theory presented in [3] and [10].

The equations of equilibrium that should be solved may be expressed as

$$\mathbf{G}(\mathbf{a}) = \mathbf{f}_{int}(\mathbf{a}) - \mathbf{f}_{ext} = \mathbf{0} \tag{33}$$

where $\mathbf{G}$ is the residual force vector (or out-of-balance force vector) and $\mathbf{f}_{int}$ is the internal force vector which both depend on the $n_{dof}$ nodal displacements $\mathbf{a}$. If constant body forces are neglected, the external forces $\mathbf{f}_{ext}$ may be expressed as

$$\mathbf{f}_{ext} = \lambda \mathbf{f} \tag{34}$$

where $\mathbf{f}$ is a fixed load pattern and where $\lambda$ is a variable load factor. The equations of equilibrium may then be expressed as

$$\mathbf{G}(\mathbf{a}, \lambda) = \mathbf{f}_{int}(\mathbf{a}) - \lambda \mathbf{f} = \mathbf{0} \tag{35}$$

which represents $n_{dof}$ equations and $n_{dof} + 1$ unknowns; the $n_{dof}$ nodal displacements and the load factor $\lambda$. To solve the above system of equations, some further relation is needed in addition to considering the essential boundary conditions. This additional relation, the constraint equation $g$, is in [3] suggested as

$$g(\mathbf{a}, \lambda) = \Delta \mathbf{a}^T \Delta \mathbf{a} + \psi \Delta \lambda^2 \mathbf{f}^T \mathbf{f} - L^2 = 0 \tag{36}$$

where $\Delta(*)$ refers to a difference between the next sought state and the previous equilibrium state, $\psi$ is a load influence factor and $L$ is the path step length. The constraint equation $g$ is
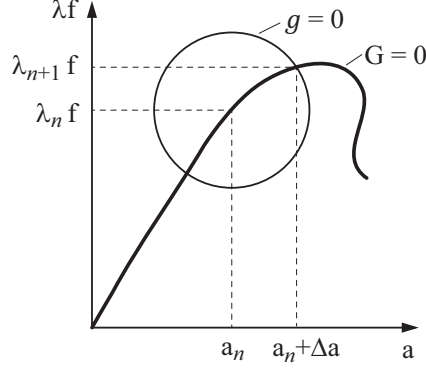
Figure 4: Illustration of constraint equation $g$ with $\psi = 1$ for a single degree of freedom system.

illustrated in Figure 4 for a single degree of freedom system. Setting $\psi = 0$ reduces some of the computational costs and does according to [10] not influence the convergence rate. An approach with $\psi = 0$ is called a cylindrical arc-length method and an approach with $\psi \neq 0$ is called a spherical arc-length method.

In analogy with the derivation of the Newton-Raphson scheme, a truncated Taylor expansion of $\mathbf{G}$ around an approximate solution $(\mathbf{a}^{i-1}, \lambda^{i-1})$ to the true solution $(\mathbf{a}, \lambda)$ yields

$$\mathbf{G}(\mathbf{a}^i, \lambda^i) = \mathbf{G}(\mathbf{a}^{i-1}, \lambda^{i-1}) + \left(\frac{\partial \mathbf{G}}{\partial \mathbf{a}}\right)^{i-1} (\mathbf{a}^i - \mathbf{a}^{i-1}) + \left(\frac{\partial \mathbf{G}}{\partial \lambda}\right)^{i-1} (\lambda^i - \lambda^{i-1}) \tag{37}$$

where the derivatives $\partial \mathbf{G}/\partial \mathbf{a} = \mathbf{K}_t$ and $\partial \mathbf{G}/\partial \lambda = -\mathrm{d}\lambda\mathbf{f}$. Enforcing equilibrium to be fulfilled according to $\mathbf{G}(\mathbf{a}^i, \lambda^i) = \mathbf{0}$ and using the notation $\mathrm{d}\mathbf{a} = \mathbf{a}^i - \mathbf{a}^{i-1}$ and $\mathrm{d}\lambda = \lambda^i - \lambda^{i-1}$ yields

$$\mathbf{K}_t^{i-1}\mathrm{d}\mathbf{a} - \mathrm{d}\lambda\mathbf{f} = -\mathbf{G}(\mathbf{a}^{i-1}, \lambda^{i-1}) \qquad \text{where} \quad \mathbf{K}_t^{i-1} = \int_\Omega \mathbf{B}^T \mathbf{D}_t^{i-1} \mathbf{B} \, \mathrm{d}\Omega \tag{38}$$

In addition to the above given equations of equilibrium, also the constraint equation should be fulfilled. There are at least two available approaches regarding this issue [10]. The constraint equation may be linearized in the same manner as the equations of equilibrium and the solution will then be forced to fulfill the constraint equation only as the solution has converged. Another approach is to enforce fulfillment of the constraint equation in every iteration, i.e. to fulfill

$$g(\mathbf{a}, \lambda) = (\Delta \mathbf{a}^i)^T \Delta \mathbf{a}^i + \psi(\Delta \lambda^i)^2 \mathbf{f}^T \mathbf{f} - L^2 = 0 \tag{39}$$

where

$$\Delta \mathbf{a}^i = \Delta \mathbf{a}^{i-1} + \mathrm{d}\mathbf{a} \tag{40}$$
$$\Delta \lambda^i = \Delta \lambda^{i-1} + \mathrm{d}\lambda \tag{41}$$

where $\Delta \mathbf{a}^i$ and $\Delta \lambda^i$ are the sought increments between the next state $i$ and the last known equilibrium state $n$ and where $\Delta \mathbf{a}^{i-1}$ and $\Delta \lambda^{i-1}$ hence are the known increments between the current state $i-1$ and the last known equilibrium state $n$. Equations (38) and (39) may be solved in the following manner. Equation (38) is multiplied from the left side by the inverse of the tangential stiffness matrix $\mathbf{K}_t$ and the term related to the load factor $\mathrm{d}\lambda$ is moved to the right side to obtain

$$\mathrm{d}\mathbf{a} = -\left(\mathbf{K}_t^{i-1}\right)^{-1} \mathbf{G}(\mathbf{a}^{i-1}, \lambda^{i-1}) + \mathrm{d}\lambda \left(\mathbf{K}_t^{i-1}\right)^{-1} \mathbf{f} \tag{42}$$

which may be written as

$$\mathrm{d}\mathbf{a} = \mathrm{d}\mathbf{a_G} + \mathrm{d}\lambda\mathrm{d}\mathbf{a_f} \tag{43}$$

and where $\mathrm{d}\mathbf{a_f}$ and $\mathrm{d}\mathbf{a_G}$ are solved from

$$\left(\mathbf{K}_t^{i-1}\right)\mathrm{d}\mathbf{a_f} = \mathbf{f} \tag{44}$$
$$\left(\mathbf{K}_t^{i-1}\right)\mathrm{d}\mathbf{a_G} = -\mathbf{G}(\mathbf{a}^{i-1}, \lambda^{i-1}) \tag{45}$$

Using $\mathrm{d}\mathbf{a}$ from Equation (43) and Equations (41) and (40) in Equation (39), the only unknown quantity is the increment in load factor $\mathrm{d}\lambda$ which can be found from

$$a_1\mathrm{d}\lambda^2 + a_2\mathrm{d}\lambda + a_3 = 0 \tag{46}$$

where

$$a_1 = \mathrm{d}\mathbf{a_f}^T\mathrm{d}\mathbf{a_f} + \psi\mathbf{f}^T\mathbf{f} \tag{47}$$
$$a_2 = 2\mathrm{d}\mathbf{a_f}^T(\Delta\mathbf{a}^{i-1} + \mathrm{d}\mathbf{a_G}) + 2\psi\Delta\lambda^{i-1}\mathbf{f}^T\mathbf{f} \tag{48}$$
$$a_3 = (\Delta\mathbf{a}^{i-1} + \mathrm{d}\mathbf{a_G})^T(\Delta\mathbf{a}^{i-1} + \mathrm{d}\mathbf{a_G}) + \psi(\Delta\lambda^{i-1})^2\mathbf{f}^T\mathbf{f} - L^2 \tag{49}$$

Since Equation (46) is quadratic, two real roots or complex roots may be found. When complex roots are found, the remedy proposed in [3] and [10] is to decrease the path step length $L$ and restart the iteration procedure from a known equilibrium point. Equation (46) may give two real solutions $\mathrm{d}\lambda^{(j)}$ ($j = 1, 2$) and the solution should then be chosen such that doubling back and following the load path already found is avoided. This can be ensured by choosing the solution $j$ which minimizes the angle between $\Delta\mathbf{a}^{i-1}$ and $\Delta\mathbf{a}^i$. This solution is the one which maximizes

$$a_4 + a_5\mathrm{d}\lambda^{(j)} \qquad \text{where } j = 1, 2 \tag{50}$$

where

$$a_4 = (\Delta\mathbf{a}^{i-1})^T(\Delta\mathbf{a}^{i-1} + \mathrm{d}\mathbf{a_G}) \tag{51}$$
$$a_5 = (\Delta\mathbf{a}^{i-1})^T\mathrm{d}\mathbf{a_f} \tag{52}$$

In addition to the cases when complex or two real roots of Equation (46) are found, special attention is also needed for the first iteration in every path step. For the fist iteration is $\Delta\lambda^{i-1} = 0$, $\Delta\mathbf{a}^{i-1} = \mathbf{0}$ and $\mathbf{G}^{i-1} = \mathbf{0}$ which gives $a_2 = 0$ according to Equation (48). Two real solutions of Equation (46) then exists and the solution is then for the general case chosen in accordance with Equations (50)-(52). For the first iteration however, this procedure offers no help since $a_4 = a_5 = 0$. The solution offered in [10] is then to apply the same general principle of minimizing the angle between two previous solutions of the nodal displacements, although now these solutions are two previous accepted equilibrium solutions and not $\Delta\mathbf{a}^{i-1}$ and $\Delta\mathbf{a}^i$ as used above. The increment in the load factor $\mathrm{d}\lambda$ is in the first iteration hence determined according to

$$\mathrm{d}\lambda = s\frac{L}{\sqrt{\mathrm{d}\mathbf{a_f}^T\mathrm{d}\mathbf{a_f} + \psi\mathbf{f}^T\mathbf{f}}} \qquad \text{where} \quad s = \mathrm{sign}(\Delta\mathbf{a}_n^T\mathrm{d}\mathbf{a_f}) \tag{53}$$

where $\Delta\mathbf{a}_n$ is taken as the increment in nodal displacements between the two last converged equilibrium points, i.e. $\Delta\mathbf{a}_n = \mathbf{a}_n - \mathbf{a}_{n-1}$.

Conventional arc-length approaches, with a constraint equation according to Equation (36), seems to be well suited for geometrically nonlinear problems but have been reported to work less satisfactory for applications including material instabilities giving localized fracture process zones [12]. Examples of such applications are fracture analyses of concrete or wooden structural elements using cohesive zone models, where the material nonlinearity commonly is confined to only a small volume of the considered body. The global solution path may for such applications include very sharp snap-backs and a constraint equation based on all nodal displacements seems for some reason insufficient to capture this phenomenon correctly. There are numerous suggestions found in the literature regarding the choice of constraint equation, two of these are presented below.

## Constraint equation based on only certain degrees of freedom

A constraint equation based on only certain degrees of freedom is in [2] suggested to be used for nonlinear fracture analysis of concrete. The constraint equation is very similar to the one given in Equation (36) with $\psi = 0$ and reads

$$g(\mathbf{a}, \lambda) = \Delta\tilde{\mathbf{a}}^T \Delta\tilde{\mathbf{a}} - L^2 = 0 \tag{54}$$

where $\tilde{\mathbf{a}}$ are the nodal displacements related to elements with material nonlinearity only. This type of approach is straightforward to implement for applications with a known, predefined volume within which the material nonlinearity is present.

## Constraint equation based on plastic energy dissipation

A rather different approach for formulation of the constraint equation is presented in [12]. The main idea of this approach is to find the equilibrium path by considering energy dissipation. For an application with strain-softening plasticity in a predefined potential fracture zone (volume) and linear elasticity for the bulk material, the formulation presented in [12] is restated below.

The rate of energy dissipation $G$ may be expressed as

$$G = P - \dot{U}_e \tag{55}$$

where $P = \dot{\mathbf{a}}^T \mathbf{f}_{ext} = \lambda\dot{\mathbf{a}}^T \mathbf{f}$ is the exerted power and $\dot{U}_e$ is the rate of elastic strain energy. The elastic energy stored in a body of volume $\Omega$ is given by

$$U_e = \frac{1}{2}\int_\Omega (\boldsymbol{\varepsilon}^e)^T \boldsymbol{\sigma} \, \mathrm{d}\Omega = \frac{1}{2}\int_\Omega \boldsymbol{\sigma}^T \mathbf{D}^{-1}\boldsymbol{\sigma} \, \mathrm{d}\Omega \tag{56}$$

where $\boldsymbol{\varepsilon}^e$ is the elastic part of the total strain $\boldsymbol{\varepsilon} = \boldsymbol{\varepsilon}^e + \boldsymbol{\varepsilon}^p$ and $\boldsymbol{\sigma} = \mathbf{D}\boldsymbol{\varepsilon}^e$ where $\mathbf{D}$ is the linear elastic material stiffness matrix. The rate of the elastic strain energy is then given by

$$\dot{U}_e = \int_\Omega \dot{\boldsymbol{\sigma}}^T \mathbf{D}^{-1}\boldsymbol{\sigma} \, \mathrm{d}\Omega = \int_\Omega \dot{\boldsymbol{\varepsilon}}^T (\mathbf{D}^{ep})^T \mathbf{D}^{-1}\boldsymbol{\sigma} \, \mathrm{d}\Omega \tag{57}$$

where $\mathbf{D}^{ep}$ is the elasto-plastic stiffness matrix which for plastic straining relates the increment in total strain to the increment in stress according to $\dot{\boldsymbol{\sigma}} = \mathbf{D}^{ep}\dot{\boldsymbol{\varepsilon}}$. Using the strain-nodal displacement relation according to Equation (11) then yields

$$\dot{U}_e = \dot{\mathbf{a}}^T \mathbf{f}^* \qquad \text{where} \qquad \mathbf{f}^* = \int_\Omega \mathbf{B}^T (\mathbf{D}^{ep})^T \mathbf{D}^{-1}\boldsymbol{\sigma} \, \mathrm{d}\Omega \tag{58}$$

The energy release rate (or rate of energy dissipation) then follows as

$$G = P - \dot{U}_e = \dot{\mathbf{a}}^T(\lambda \mathbf{f} - \mathbf{f}^*) \tag{59}$$

which is used to formulate the following constraint equation

$$g(\mathbf{a}, \lambda) = \Delta \mathbf{a}^T(\lambda_n \mathbf{f} - \mathbf{f}_n^*) - L = 0 \tag{60}$$

where $\lambda_n$ and $\mathbf{f}_n^*$ refer to converged quantities from the last equilibrium state. The solution procedure for direct consideration of the dissipation-based constraint equation is the same as for the conventional arc-length approach presented above: Equations (40) - (45) are used and the constraint equation is enforced to be fulfilled in every iteration according to

$$g(\mathbf{a}, \lambda) = (\Delta \mathbf{a}^i)^T(\lambda_n \mathbf{f} - \mathbf{f}_n^*) - L = 0 \tag{61}$$

and the increment in the load factor $\mathrm{d}\lambda$ may then be determined from

$$\mathrm{d}\lambda = \frac{L - (\Delta \mathbf{a}^{i-1} + \mathrm{d}\mathbf{a_G})^T(\lambda_n \mathbf{f} - \mathbf{f}_n^*)}{\mathrm{d}\mathbf{a_f}^T(\lambda_n \mathbf{f} - \mathbf{f}_n^*)} \tag{62}$$

Use of a constraint equation based on energy dissipation will for natural reasons not work properly for non-dissipative parts of the load path, i.e. before any plastic straining has taken place since then $\lambda_n \mathbf{f} = \mathbf{f}_n^*$. Implementation of a solution approach including a dissipation based constraint equation hence needs to be accompanied by an alternative solution approach, such as a conventional arc-length approach or a conventional Newton-Raphson approach, and an appropriate switching criterion.

## 5  Integration of constitutive relations

The above considered approaches for solution of the nonlinear equations of equilibrium are based on the assumption that the current stress may be determined in some way for all states along the load path. For a general elasto-plastic material, with a constitutive relation expressed in incremental form, the stress is determined by integration of the constitutive relation along the load path. Depending on the specific material model, the constitutive relation may be possible to integrate exactly but approximate solutions based on numerical integration are commonly needed. As for the solution of the global equations of equilibrium, there are several strategies available for numerical integration of incremental constitutive relations.

When solving the global equations of equilibrium in an iterative manner, the internal force vector $\mathbf{f}_{int}$ and hence also the current stresses need to be established in every iteration. From the solution of the global equations, the nodal displacements $\mathbf{a}$ are known and hence also the total strain $\boldsymbol{\varepsilon}$. What remains to determine is how much of the total strain that is elastic and how much is plastic. The following presentation is based on theory presented in [9], where methods are presented for general elasto-plastic material models. The application considered here is to a specific elasto-plastic material model for cohesive perpendicular to grain fracture of wood presented in [4]. All quantities are here expressed in a global $xyz$ coordinate system and additive decomposition of strains is assumed according to

$$\boldsymbol{\varepsilon} = \boldsymbol{\varepsilon}^e + \boldsymbol{\epsilon}^p \tag{63}$$

where $\boldsymbol{\varepsilon}$ is the total strain while $\boldsymbol{\varepsilon}^e$ and $\boldsymbol{\varepsilon}^p$ are the elastic and plastic strains respectively. Hooke's law states that

$$\boldsymbol{\sigma} = \mathbf{D}\boldsymbol{\varepsilon}^e \qquad \text{or} \qquad \dot{\boldsymbol{\sigma}} = \mathbf{D}\dot{\boldsymbol{\varepsilon}}^e \tag{64}$$

where $\mathbf{D}$ is the elastic stiffness matrix and where

$$\boldsymbol{\sigma} = \begin{bmatrix} \sigma_{xx} & \sigma_{yy} & \sigma_{zz} & \tau_{xy} & \tau_{xz} & \tau_{yz} \end{bmatrix}^T \tag{65}$$

$$\boldsymbol{\varepsilon} = \begin{bmatrix} \varepsilon_{xx} & \varepsilon_{yy} & \varepsilon_{zz} & \gamma_{xy} & \gamma_{xz} & \gamma_{yz} \end{bmatrix}^T \tag{66}$$

## 5.1 A 3D wood cohesive zone model based on plasticity theory

The material model presented in [4] is aimed at describing the material behavior within a fracture process zone, from start of strain softening at initiation of plastic straining to the creation of new traction-free surfaces. It is indented to be used within a predefined potential crack plane, which in the current implementation is forced to be oriented in the $xz$-plane and having a small height $h$ in the $y$-direction as illustrated in Figure 5. In the FE-discretization, the predefined crack plane consists of one layer of elements.

The Tsai-Wu criterion [11] is used as criterion for initiation of yielding, i.e. the formation of a fracture process zone and initiation of softening. An initial yield function $F$ is hence defined according to

$$F(\boldsymbol{\sigma}) = \boldsymbol{\sigma}^T \mathbf{q} + \boldsymbol{\sigma}^T \mathbf{P} \boldsymbol{\sigma} - 1 \quad \text{where} \quad \begin{cases} F < 0 & \text{elastic response} \\ F = 0 & \text{initiation of softening} \end{cases} \tag{67}$$

where $\mathbf{q}$ and $\mathbf{P}$ are given by material strength properties. The post softening-initiation performance is assumed to be governed by the three out-of-fracture plane stress and plastic deformation components. As softening has initiated, the yield function is changed accordingly and an updated yield function is defined as

$$f(\boldsymbol{\sigma}, K) = \sigma_{yy}^2 F_{yyyy} + \tau_{xy}^2 F_{xyxy} + \tau_{yz}^2 F_{yzyz} - K^2 \quad \text{where} \quad \begin{cases} f < 0 & \text{elastic response} \\ f = 0 & \text{elasto-plastic response} \end{cases} \tag{68}$$

where $F_{yyyy}$, $F_{xyxy}$ and $F_{yzyz}$ are yield parameters determined from the stress state at initiation of softening and $K$ is a softening parameter. Using matrix notation, the updated yield function may also be expressed as

$$f(\boldsymbol{\sigma}, K) = \boldsymbol{\sigma}^T \mathbf{R} \boldsymbol{\sigma} - K^2 \tag{69}$$

where $\mathbf{R}$ is a $6 \times 6$ matrix with $R_{22} = F_{yyyy}$, $R_{44} = F_{xyxy}$ and $R_{66} = F_{yzyz}$ and all other components equal to zero. A plastic flow rule is adopted according to

$$\dot{\boldsymbol{\varepsilon}}^p = \dot{\lambda} \frac{\partial g}{\partial \boldsymbol{\sigma}} = \dot{\lambda} \frac{\partial f}{\partial \boldsymbol{\sigma}} \quad \text{with } \dot{\lambda} \geq 0 \text{ and where} \quad \begin{cases} \dot{\lambda} = 0 & \text{elastic strains only} \\ \dot{\lambda} > 0 & \text{plastic strains} \end{cases} \tag{70}$$

where $\dot{\lambda}$ is the plastic multiplier and where $g = f$, meaning that the flow rule is associated with respect to the updated yield function $f$.
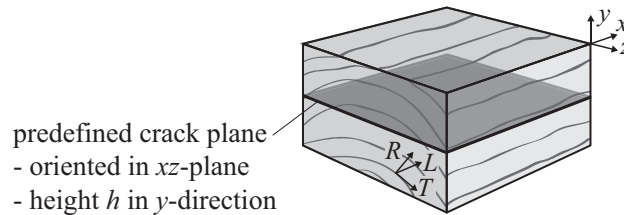


predefined crack plane
- oriented in $xz$-plane
- height $h$ in $y$-direction

Figure 5: Orientation of predefined crack plane.

The change in size of the yield surface is described by the softening parameter $K$ which is a function of an internal variable denoted the effective dimensionless deformation $\delta_{eff}$. The following softening function is adopted in [4]

$$K = \begin{cases} (1 - \delta_{eff} + c^{1/m}\delta_{eff})^m & \text{for} \quad \delta_{eff} < 1 \\ 0 & \delta_{eff} \geq 1 \end{cases} \tag{71}$$

where $m$ and $c$ are model parameters and where $K = 0$ corresponds to zero stress transferring capacity and the creation of new traction-free surfaces. A slightly different softening function is adopted for the numerical analyses in [5] and [6]. The effective dimensionless deformation $\delta_{eff}$ is expressed in plastic deformations $\delta_{yy}$, $\delta_{xy}$ and $\delta_{yz}$ and the evolution law for the internal variable is defined as

$$\dot{\delta}_{eff} = \sqrt{\left(\frac{\dot{\delta}_{yy}}{A_{yy}}\right)^2 + \left(\frac{\dot{\delta}_{xy}}{A_{xy}}\right)^2 + \left(\frac{\dot{\delta}_{yz}}{A_{yz}}\right)^2} \tag{72}$$

where $A_{yy}$, $A_{xy}$ and $A_{yz}$ are scaling parameters of dimension length related to the fracture energies in the three corresponding modes of deformation. The increments in plastic deformation are determined according to $\dot{\delta}_{yy} = h\dot{\varepsilon}_{yy}^p$, $\dot{\delta}_{xy} = h\dot{\gamma}_{xy}^p$ and $\dot{\delta}_{yz} = h\dot{\gamma}_{yz}^p$ by assuming constant plastic strains over the small out-of-plane ($y$-direction) height $h$ of the predefined crack plane. Using Equation (70), the evolution law for the internal variable $\delta_{eff}$ may then be expressed as

$$\dot{\delta}_{eff} = \dot{\lambda}k \quad \text{where} \quad k = 2h\sqrt{\left(\frac{\sigma_{yy}F_{yyyy}}{A_{yy}}\right)^2 + \left(\frac{\tau_{xy}F_{xyxy}}{A_{xy}}\right)^2 + \left(\frac{\tau_{yz}F_{yzyz}}{A_{yz}}\right)^2} \tag{73}$$

where $k$ is the evolution function for the internal variable.

## 5.2 Numerical integration of constitutive relations

With the relevant relations of the material model defined above, attention will now be paid to the process of determining the stress state along the load path. In the following description, the previous equilibrium state where all quantities are known will be denoted state 1 while the updated state for which the stress is sought will be denoted state 2. Accordingly, quantities related to the two states are denoted $(*)_1$ and $(*)_2$ respectively. While all quantities are known at state 1, only the nodal displacements and hence the total strain $\varepsilon_2$ are known at the state 2. Using Equations (63) and (64), the stress at state 1 and state 2 may be expressed as

$$\boldsymbol{\sigma}_1 = \mathbf{D}\left(\boldsymbol{\varepsilon}_1 - \boldsymbol{\varepsilon}_1^p\right) \tag{74}$$

$$\boldsymbol{\sigma}_2 = \mathbf{D}\left(\boldsymbol{\varepsilon}_2 - \boldsymbol{\varepsilon}_2^p\right) \tag{75}$$

which by subtraction, rearrangement and expressing the difference in total strain and in plastic strain as $\Delta\boldsymbol{\varepsilon} = \boldsymbol{\varepsilon}_2 - \boldsymbol{\varepsilon}_1$ and $\Delta\boldsymbol{\varepsilon}^p = \boldsymbol{\varepsilon}_2^p - \boldsymbol{\varepsilon}_1^p$ respectively yields

$$\boldsymbol{\sigma}_2 = \boldsymbol{\sigma}_1 + \mathbf{D}\Delta\boldsymbol{\varepsilon} - \mathbf{D}\Delta\boldsymbol{\varepsilon}^p \tag{76}$$

where $\Delta\boldsymbol{\varepsilon}^p$ is to be determined by some type of integration of Equation (70) in order to find $\boldsymbol{\sigma}_2$. For further elaboration it is convenient to define a trial stress $\boldsymbol{\sigma}_t$ according to

$$\boldsymbol{\sigma}_t = \boldsymbol{\sigma}_1 + \mathbf{D}\Delta\boldsymbol{\varepsilon} \tag{77}$$

14

and hence such that the trial stress equals the sought stress $\boldsymbol{\sigma}_2$ if the change in nodal displacements results in a change of strain that is purely elastic, i.e. $\Delta\boldsymbol{\varepsilon} = \Delta\boldsymbol{\varepsilon}^e$ and $\Delta\boldsymbol{\varepsilon}^p = \mathbf{0}$. The stress state is required to be located inside or on the yield surface in the stress space, i.e. the condition $f(\boldsymbol{\sigma}, K) \leq 0$ must always hold. The *consistency relation* states that during plastic loading accompanied by a change in stress state, also the softening parameters vary in such a way that the stress state always remains on the yield surface [9]. For purely elastic loading however, the softening parameters and hence also the yield surface is unchanged. The trial stress may be used as a tool to check for elasto-plastic response according to

- if $f(\boldsymbol{\sigma}_t, K_1) \leq 0 \quad \Rightarrow \quad \begin{cases} \text{elastic response:} \\ \boldsymbol{\sigma}_2 = \boldsymbol{\sigma}_t, \ K_2 = K_1, \ \delta_{eff,2} = \delta_{eff,1} \end{cases}$

- else $\quad\quad\quad\quad\quad \Rightarrow \quad \begin{cases} \text{elasto-plastic response:} \\ \boldsymbol{\sigma}_2, \ K_2, \ \delta_{eff,2} \text{ determined by numerical integration} \end{cases}$

The method for numerical integration of the incremental constitutive relation considered in this section is the *fully implicit (backward Euler) return method* [9], a so called *direct method* based on the *generalized mid-point rule*. The integration of the flow rule in Equation (70) and the evolution law for the internal variable in Equation (73) is performed in an approximate manner according to

$$\dot{\boldsymbol{\varepsilon}}^p = \dot{\lambda}\frac{\partial g}{\partial \boldsymbol{\sigma}} \quad \Rightarrow \quad \Delta\boldsymbol{\varepsilon}^p = \int_{\lambda_1}^{\lambda_1+\Delta\lambda} \frac{\partial g}{\partial \boldsymbol{\sigma}} \, \mathrm{d}\lambda \approx \Delta\lambda\left(\frac{\partial g}{\partial \boldsymbol{\sigma}}\right)_2 \tag{78}$$

$$\dot{\delta}_{eff} = \dot{\lambda}k \quad \Rightarrow \quad \Delta\delta_{eff} = \int_{\lambda_1}^{\lambda_1+\Delta\lambda} k \, \mathrm{d}\lambda \approx \Delta\lambda k_2 \tag{79}$$

where index 2 indicates that $\partial g/\partial\boldsymbol{\sigma}$ and $k$ are evaluated at state 2. This results in the following set of 6+1+1 nonlinear equations

$$\boldsymbol{\sigma}_2 = \boldsymbol{\sigma}_t - \mathbf{D}\left(\partial g/\partial\boldsymbol{\sigma}\right)_2 \Delta\lambda \tag{80}$$
$$f(\boldsymbol{\sigma}_2, K_2) = 0 \tag{81}$$
$$K_2 = \left(1 - (\delta_{eff,1} + \Delta\lambda k_2) + c^{1/m}(\delta_{eff,1} + \Delta\lambda k_2)\right)^m \tag{82}$$

which should be solved for the 8 unknowns: the six stress components of $\boldsymbol{\sigma}$, the softening parameter $K$ and the plastic multiplier $\Delta\lambda$. An iterative solution approach based on the Newton-Raphson method is used. A vector $\mathbf{S}$ containing the sought stress components and the plastic multiplier and a residual vector $\mathbf{V}$ are defined according to

$$\mathbf{S}^i = \begin{bmatrix} \boldsymbol{\sigma}^i \\ \Delta\lambda^i \end{bmatrix} \quad \text{and} \quad \mathbf{V}^i = \begin{bmatrix} \mathbf{V}_\sigma^i \\ V_f^i \end{bmatrix} = \begin{bmatrix} \boldsymbol{\sigma}^i + \Delta\lambda^i\mathbf{D}(\frac{\partial g}{\partial \boldsymbol{\sigma}})^i - \boldsymbol{\sigma}_t \\ f(\boldsymbol{\sigma}^i, K^i) \end{bmatrix} \tag{83}$$

where $i$ indicates quantities in iteration $i$. The sought solution is defined by $\mathbf{V}(\mathbf{S}) = \mathbf{0}$ and is found by an iterative procedure according to

$$\mathbf{S}^i = \mathbf{S}^{i-1} - \left[\frac{\partial \mathbf{V}^{i-1}}{\partial \mathbf{S}}\right]^{-1} \mathbf{V}^{i-1} \tag{84}$$

where the iteration matrix $\partial\mathbf{V}/\partial\mathbf{S}$ for the present material model may be reduced from the expressions given in [9] for a general plasticity model as

$$\frac{\partial \mathbf{V}}{\partial \mathbf{S}} = \begin{bmatrix} \mathbf{I}_6 + \Delta\lambda\mathbf{D}\frac{\partial^2 g}{\partial\boldsymbol{\sigma}\partial\boldsymbol{\sigma}} & \mathbf{D}\frac{\partial g}{\partial\boldsymbol{\sigma}} \\ \left(\frac{\partial f}{\partial\boldsymbol{\sigma}}\right)^T & 0 \end{bmatrix} \tag{85}$$

15

where $\mathbf{I}_6$ denote a $6 \times 6$ identity matrix and where

$$\frac{\partial g}{\partial \boldsymbol{\sigma}} = \frac{\partial f}{\partial \boldsymbol{\sigma}} = 2\mathbf{R}\boldsymbol{\sigma} \quad \text{and} \quad \frac{\partial^2 g}{\partial \boldsymbol{\sigma} \partial \boldsymbol{\sigma}} = 2\mathbf{R} \tag{86}$$

For the first iteration ($i = 1$), the starting quantities for the iteration procedure are given by $\boldsymbol{\sigma}^0 = \boldsymbol{\sigma}_t$ and $\Delta\lambda^0 = 0$ yielding

$$\mathbf{S}^0 = \begin{bmatrix} \boldsymbol{\sigma}_t \\ 0 \end{bmatrix} \quad \text{and} \quad \mathbf{V}^0 = \begin{bmatrix} \mathbf{0} \\ f(\boldsymbol{\sigma}_t, K_1) \end{bmatrix} \tag{87}$$

The softening parameter $K$ is in every iteration $i$ determined according to

$$K^i = \left(1 - \delta^i_{eff} + c^{1/m}\delta^i_{eff}\right)^m \quad \text{where } \delta^i_{eff} = \delta_{eff,1} + \Delta\delta^i_{eff} = \delta_{eff,1} + \Delta\lambda^i k^i \tag{88}$$

where the index $i$ indicates that $\Delta\lambda^i$ is obtained from Equation (84) in iteration $i$ and that $k$ is evaluated using the stress $\boldsymbol{\sigma}^i$ obtained in the same manner.

Due to the change from the initial yield function $F$ to the updated yield function $f$ and the nature of the incremental solution, special attention needs to be paid to the integration of constitutive relations at initiation of yielding. The issue concerns the parameters $F_{yyyy}$, $F_{xyxy}$ and $F_{yzyz}$ which define the updated yield function $f$ and which are unknown in the beginning of the load step where plastic straining is first initiated. This may be solved by approximating these parameters at initiation of yielding according to

$$F_{yyyy} \approx P_{22} , \quad F_{xyxy} \approx P_{44} , \quad F_{yzyz} \approx P_{66} \tag{89}$$

where $P_{ii}$ ($i = 2, 4, 6$) denotes three diagonal components of the matrix $\mathbf{P}$. The derivate $\partial f/\partial \boldsymbol{\sigma}$ in Equation (85) is however taken as $\partial F/\partial \boldsymbol{\sigma}$ since the stress should be bound to the initial yield surface $F$. The parameters $F_{yyyy}$, $F_{xyxy}$ and $F_{yzyz}$ used for subsequent computations are then determined such that the two yield surfaces $f$ and $F$ intersect at the accepted equilibrium stress state $\boldsymbol{\sigma}_c$ at which softening is initialized according to

$$F(\boldsymbol{\sigma}_c) = f(\boldsymbol{\sigma}_c, K = 1) = 0 \tag{90}$$

and the considered parameters may then be determined according to

$$F_{yyyy} = P_{22}/\left(\sigma^2_{c,yy}P_{22} + \tau^2_{c,xy}P_{44} + \tau^2_{c,yz}P_{66}\right) \tag{91}$$

$$F_{xyxy} = P_{44}/\left(\sigma^2_{c,yy}P_{22} + \tau^2_{c,xy}P_{44} + \tau^2_{c,yz}P_{66}\right) \tag{92}$$

$$F_{yzyz} = P_{66}/\left(\sigma^2_{c,yy}P_{22} + \tau^2_{c,xy}P_{44} + \tau^2_{c,yz}P_{66}\right) \tag{93}$$

The flow rule is hence actually non-associated in the load step were plastic straining is initiated and a small error, related to the path step length, may be introduced. Some further comments on this matter are found in [4].

# 6    Some comments regarding numerical implementation

The cohesive zone model briefly presented in Section 5, and more thoroughly presented in [4], has been implemented for nonlinear finite element analysis using solution approaches presented in Sections 4 and 5. The implementation was carried out in MATLAB [7] using supplementary routines from the toolbox CALFEM [1]. The material model has been applied to analysis of double

cantilever beam specimens and end-notched beams using a cylindrical arc-length approach with a conventional constraint equation [4] and analysis of glulam beams with a hole using an arc-length approach with a constraint equation based on energy dissipation [5]. Further analyses include studies of dowel-type connections, using a Newton-Raphson approach and using a cylindrical arc-length approach with a constraint equation considering only certain degrees of freedom [6]. Pseudo codes for the arc-length method are given in Section 6.1 for a conventional type of constraint equation and in Section 6.2 for an energy dissipation based constraint equation.

For the applications of the material model presented in [4], [5] and [6], the nonlinear softening performance is restricted to a predefined potential crack plane and linear elastic behavior is assumed for the bulk material. This allows for some simple but rather efficient ways to reduce the computational cost. Since the stiffness contributions from the linear elastic elements to the global tangential stiffness matrix are constant, these contributions need to be determined and assembled only once for each analysis. The residual force vector will furthermore only have non-zero components for the degrees of freedom associated with elements showing nonlinear behavior, i.e. the degrees of freedom associated with the predefined crack plane. If the major interest is some global load vs. displacement relation, determination of stresses is hence only necessary for the elements within the predefined crack plane and for linear elastic elements sharing nodes with the elements within the crack plane.

The conventional formulation of the arc-length method suffers from the drawback that complex solutions may be found when solving Equation (46) to find the increment in load factor $d\lambda$. The remedy for this problem proposed in [3] and [10] is to restart the iteration procedure from the last know equilibrium point using a smaller value of the prescribed path step length $L$. This does however not guarantee that real roots and convergence are eventually found. There are also more complex strategies for avoiding the complex roots suggested in the literature. Numerical problems may also be manifested by divergence of the procedure for the numerical integration of constitutive relations according to Equation (84).

The experience from the work presented in [4], [5] and [6] is that numerical problems sometimes can be avoided be restarting the iteration process not from the last equilibrium state, but from a few states back and temporarily adjusting the tolerance limit for the convergence criteria and/or adjusting the path step length. Also simply increasing the path step length $L$ temporarily has been found to solve the problem of finding complex roots for the increment in load factor $d\lambda$. The solution should however be checked such that the obtained loading path does not deviate from the expected loading path, i.e. such that an equilibrium path with elastic unloading is followed when the sought equilibrium path should correspond to continuous crack propagation.

For analyses of glulam beams loaded in bending and containing a hole, numerical problems were for large beams sometimes encountered when considered softening within two separate crack planes. These problems are believed to be related to simultaneous unloading (crack closure) within one crack plane and crack propagation within the other. See [5] for further comments regarding this matter.

Criteria for acceptance of global equilibrium and convergence are of importance for nonlinear analyses. Within the numerical work relating to the considered cohesive zone model has the following convergence criterion been used

$$\sqrt{\mathbf{G}^T\mathbf{G}} < \epsilon_G F_{tot} \tag{94}$$

where $\mathbf{G}$ is the residual force vector (the out-of-balance force vector), $F_{tot}$ is the total applied external load and $\varepsilon_G$ is the tolerance limit. For the analyses presented in [4], [5] and [6], values of $\varepsilon_G$ between $10^{-3}$ and $10^{-5}$ have been used.

## 6.1 Arc-length method with a conventional constraint equation

A pseudo code for the arc-length method with a conventional constraint equation is outlined in the box below. The pseudo code is valid also for a constraint equation based on only a limited number of degrees of freedom, whereby all quantities related to the nodal displacements in the constraint equation are determined from the reduced vector $\tilde{\mathbf{a}}$ instead of the full vector $\mathbf{a}$.

---

**Arc-length method with a conventional constraint equation**

*For path step $n = 1, 2, 3, \ldots, n_{max}$*

- *Initiate iteration quantities from accepted equilibrium quantities*

  $\mathbf{a}^0 = \mathbf{a}_{n-1}$ , $\lambda^0 = \lambda_{n-1}$ , $\boldsymbol{\sigma}_1 = \boldsymbol{\sigma}_2$ , $K_1 = K_2$ , $\delta_{eff,1} = \delta_{eff,2}$

- *Equilibrium iterations $i = 1, 2, \ldots$ while $\|\mathbf{G}\| >$ tolerance*

  · *calculate elasto-plastic stiffness and assemble global tangential stiffness*

  $\mathbf{D}^{ep}, \mathbf{K}_t \quad \Leftarrow \quad (\boldsymbol{\sigma}_2, K_2, \delta_{eff,2}, \mathbf{D}, \mathbf{q}, \mathbf{P}, \mathbf{R}, \text{mesh geometry and topology})$

  · *calculate pseudo displacements from*

  $\mathbf{K}_t \mathrm{d}\mathbf{a_f} = \mathbf{f}$ and $\mathbf{K}_t \mathrm{d}\mathbf{a_G} = -\mathbf{G}$

  · *calculate load factor*

  *if $i = 1$*

  $\mathrm{d}\lambda = sL / \sqrt{\mathrm{d}\mathbf{a_f}^T \mathrm{d}\mathbf{a_f} + \psi \mathbf{f}^T \mathbf{f}}$ where $s = \mathrm{sign}(\Delta \mathbf{a}_n^T \mathrm{d}\mathbf{a_f})$

  *else*

  *determine $a_1$, $a_2$, $a_3$ and solve $\mathrm{d}\lambda$ from $a_1 \mathrm{d}\lambda^2 + a_2 \mathrm{d}\lambda + a_3 = 0$*

  *if two real solutions, take special care*

  *if complex solutions, restart iteration*

  $\lambda^i = \lambda^{i-1} + \mathrm{d}\lambda$

  · *calculate nodal displacements*

  $\mathrm{d}\mathbf{a} = \mathrm{d}\mathbf{a_G} + \mathrm{d}\lambda \mathrm{d}\mathbf{a_f}$

  $\mathbf{a}^i = \mathbf{a}^{i-1} + \mathrm{d}\mathbf{a}$

  · *calculate element strains*

  $\Delta \boldsymbol{\varepsilon} = \mathbf{B}(\mathbf{a}^i - \mathbf{a}^0)$

  · *calculate element stresses according to Section 5*

  $\boldsymbol{\sigma}_2, K_2, \delta_{eff,2} \quad \Leftarrow \quad (\Delta \boldsymbol{\varepsilon}, \boldsymbol{\sigma}_1, K_1, \delta_{eff,1}, \mathbf{D}, \mathbf{q}, \mathbf{P}, \mathbf{R})$

  · *calculate residual force vector from internal and external force vectors*

  $\mathbf{G} = \mathbf{f}_{int} - \mathbf{f}_{ext}$ where $\mathbf{f}_{int} = \int_\Omega \mathbf{B}^T \boldsymbol{\sigma}_2 \, \mathrm{d}\Omega$ and $\mathbf{f}_{ext} = \lambda^i \mathbf{f}$

  *restart iteration if global or local divergence*

- *For elements with initialization of softening during path step $n$ :*

  *switch from initial to updated yield function*

  $\mathbf{R} \quad \Leftarrow \quad (K_2, K_1, \boldsymbol{\sigma}_2, \mathbf{q}, \mathbf{P})$

- *Accept iteration quantities*

  $\lambda_n = \lambda^i$ , $\mathbf{a}_n = \mathbf{a}^i$

---

## 6.2 Arc-length method with a dissipation based constraint equation

A pseudo code for the arc-length method with a constraint equation based on energy dissipation is outlined in the box below. Due to the nature of the constraint equation, being based on consideration of energy dissipation by plastic straining, the method is only applicable once plastic straining of the material has taken place. The pseudo code below takes it start in the accepted equilibrium quantities of path step $n_{dis}$, during which plastic straining is first initialized.

---

**Arc-length method with a dissipation based constraint equation**

*For path step $n = n_{dis} + 1, n_{dis} + 2, \ldots, n_{max}$*

- *Initiate iteration quantities from accepted equilibrium quantities*
  $$\mathbf{a}^0 = \mathbf{a}_{n-1} \ , \quad \lambda^0 = \lambda_{n-1} \ , \quad \boldsymbol{\sigma}_1 = \boldsymbol{\sigma}_2 \ , \quad K_1 = K_2 \ , \quad \delta_{eff,1} = \delta_{eff,2}$$

- *Calculate pseudo force vector*
  $$\mathbf{f}_n^* = \int_\Omega \mathbf{B}^T (\mathbf{D}^{ep})^T \mathbf{D}^{-1} \boldsymbol{\sigma}_2 \ \mathrm{d}\Omega$$

- *Equilibrium iterations $i = 1, 2, \ldots$ while $\|\mathbf{G}\| >$ tolerance*
  - *calculate elasto-plastic stiffness and assemble global tangential stiffness*
    $$\mathbf{D}^{ep}, \mathbf{K}_t \quad \Leftarrow \quad (\boldsymbol{\sigma}_2, K_2, \delta_{eff,2}, \mathbf{D}, \mathbf{q}, \mathbf{P}, \mathbf{R}, \text{mesh geometry and topology})$$
  - *calculate pseudo displacements from*
    $$\mathbf{K}_t \mathrm{d}\mathbf{a_f} = \mathbf{f} \quad \text{and} \quad \mathbf{K}_t \mathrm{d}\mathbf{a_G} = -\mathbf{G}$$
  - *calculate load factor*
    $$\mathrm{d}\lambda = \frac{L - (\Delta \mathbf{a}^{i-1} + \mathrm{d}\mathbf{a_G})^T (\lambda^0 \mathbf{f} - \mathbf{f}_n^*)}{\mathrm{d}\mathbf{a_f}^T (\lambda^0 \mathbf{f} - \mathbf{f}_n^*)} \qquad \text{where} \quad \Delta \mathbf{a}^{i-1} = \mathbf{a}^{i-1} - \mathbf{a}^0$$
    $$\lambda^i = \lambda^{i-1} + \mathrm{d}\lambda$$
  - *calculate nodal displacements*
    $$\mathrm{d}\mathbf{a} = \mathrm{d}\mathbf{a_G} + \mathrm{d}\lambda \mathrm{d}\mathbf{a_f}$$
    $$\mathbf{a}^i = \mathbf{a}^{i-1} + \mathrm{d}\mathbf{a}$$
  - *calculate element strains*
    $$\Delta \boldsymbol{\varepsilon} = \mathbf{B}(\mathbf{a}^i - \mathbf{a}^0)$$
  - *calculate element stresses according to Section 5*
    $$\boldsymbol{\sigma}_2, K_2, \delta_{eff,2} \quad \Leftarrow \quad (\Delta \boldsymbol{\varepsilon}, \boldsymbol{\sigma}_1, K_1, \delta_{eff,1}, \mathbf{D}, \mathbf{q}, \mathbf{P}, \mathbf{R})$$
  - *calculate residual force vector from internal and external force vectors*
    $$\mathbf{G} = \mathbf{f}_{int} - \mathbf{f}_{ext} \quad \text{where} \quad \mathbf{f}_{int} = \int_\Omega \mathbf{B}^T \boldsymbol{\sigma}_2 \ \mathrm{d}\Omega \ \text{ and } \ \mathbf{f}_{ext} = \lambda^i \mathbf{f}$$
    *restart iteration if global or local divergence*

- *For elements with initialization of softening during path step $n$ :*
  *switch from initial to updated yield function*
  $$\mathbf{R} \quad \Leftarrow \quad (K_2, K_1, \boldsymbol{\sigma}_2, \mathbf{q}, \mathbf{P})$$

- *Accept iteration quantities*
  $$\lambda_n = \lambda^i \ , \quad \mathbf{a}_n = \mathbf{a}^i$$

---

# References

[1] Austrell PE, Dahlblom O, Lindemann J et al. (2004) CALFEM – A finite element toolbox. Version 3.4, Division of Structural Mechanics, Lund University, Sweden.

[2] de Borst R (1987) Computation of post-bifurcation and post-failure behavior of strain-softening solids. Computers and Structures, 25:221-224.

[3] Crisfield MA (1991) Nonlinear finite element analysis of solids and structures – Volume 1. John Wiley & Sons Ltd, Chichester, Great Britain.

[4] Danielsson H, Gustafsson PJ (2013) A three dimensional plasticity model for perpendicular to grain cohesive fracture in wood. Engineering Fracture Mechanics, 98:137-152.

[5] Danielsson H, Gustafsson PJ. Fracture analysis of glulam beams with a hole using a 3D cohesive zone model.
Submitted for publication

[6] Danielsson H, Gustafsson PJ. Fracture analysis of perpendicular to grain loaded dowel-type connections using a 3D cohesive zone model.
Submitted for publication

[7] Matlab. The Mathworks, Inc.

[8] Ottosen NS, Petersson H (1992) Introduction to the finite element method. Prentice Hall, Great Britain.

[9] Ottosen NS, Ristinmaa M (2005) The mechanics of constitutive modeling. Elsevier, Great Britain.

[10] Ristinmaa M, Ljung C (1998) An introduction to stability analysis. Division of Solid Mechanics, Lund University, Sweden.

[11] Tsai SW, Wu EM (1971) A general theory of the strength of anisotropic materials. Journal of Composite Materials, 5:58-80.

[12] Verhoosel CV, Remmers JJC, Gutiérrez MA (2009) A dissipation based arc-length method for robust simulation of brittle and ductile failure. International Journal for Numerical Methods in Engineering, 77:1290-1321.